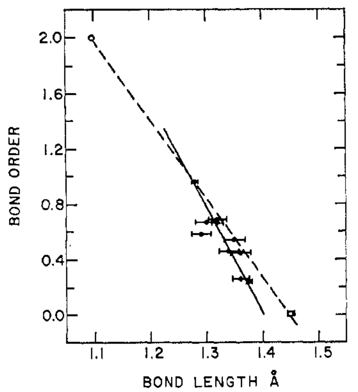

Figure 6.—Bond order as a function of bond length: - - -, predicted on the basis of N≡N = 1.097 Å and N—N = 1.449 Å; —, empirical relation.

A rationalization may be presented for the observed N—N bond lengths. The bond order (η) for the π system for two N—N bonds in the N_4B ring was calculated by a simple Hückel LCAO–MO method, with ω technique, to be 0.94 and 0.24. Results of similar MO calculations for other 6π-electron rings which contain N—N bonds are tabulated in Table V. While one may question the quantitative significance in these calculations, it is interesting to note that the empirical relation

$$\text{N-N} = 1.403 - 0.128\eta_{\text{N-N}}\ \text{Å}$$

correlates the N—N bond lengths and the bond orders within the experimental error. As shown in Figure 6 the bond lengths in these rings are shorter than predicted on a basis of N≡N = 1.097 Å in N_2[25] and N—N = 1.449 Å in N_2H_4[17] (broken line in the figure). The $(2 + 4n)$ rule is satisfied by $(CH_3)_2N_4BH$ for $n = 1$ if one does not count the nonbonding electron pairs on the doubly bonded N atoms and for $n = 2$ if one does include them.

Acknowledgments.—The authors wish to thank Dr. J. H. Morris for providing samples of this new compound, Mr. M. Cardillo for help in taking the photographs, and Mr. R. Hilderbrandt for developing some of the computer programs. The electron diffraction study was supported by the Advanced Research Projects Agency, the Army Research Office (Durham), and the National Science Foundation.

(25) P. G. Wilkinson and N. B. Houk, *J. Chem. Phys.*, **24**, 528 (1956).

CONTRIBUTION FROM THE DEPARTMENT OF CHEMISTRY,
CORNELL UNIVERSITY, ITHACA, NEW YORK 14850

The Structure of Borazine

BY W. HARSHBARGER, G. LEE, R. F. PORTER, AND S. H. BAUER

Received January 8, 1969

The molecular structure of borazine ($B_3N_3H_6$) was reinvestigated by electron diffraction. A planar D_{3h} model and two nonplanar (C_{3v} and C_2) models were fitted to the diffraction data. For two sets of data the nonplanar models statistically fit the observed diffraction data better than did the planar model. Owing to the absence of a permanent dipole moment for borazine, the C_2 model or a D_{3h} model with very large vibrational motion is preferred; the choice between these is not unambiguous. The bonded distances are B–N = 1.4355 ± 0.0021 Å, B–H = 1.258 ± 0.014 Å, and N–H = 1.050 ± 0.012 Å. The ring angles are ∠NBN = 117.7 ± 1.2° and ∠BNB = 121.1 ± 1.2°.

Introduction

The molecular structure of borazine in the gas phase was investigated previously by electron diffraction.[1,2] The conclusion of those studies, in which the visual technique was used, was that the molecule consisted of a planar ring with a B–N bond distance of 1.44 ± 0.02 Å.[2] A redetermination of the structure of borazine was undertaken to obtain more precise values for the interatomic distances, utilizing the greatly improved techniques which have been developed during the past three decades.

A large number of data, relevant to a discussion of its molecular structure, are now available on the physical properties of borazine. Since this compound is isoelectronic with and structurally similar to benzene, many investigators considered the question of the degree of electron delocalization which should be used to describe the p–π electron system of borazine. The B–N bond length is significantly shorter in $B_3N_3H_6$ than the 1.56 Å found in crystalline borazane, H_3BNH_3,[3] pointing to a higher bond order in borazine. Polarization measurements[4,5] appeared to indicate that this compound has a finite electric dipole moment, contradicting the symmetric planar structure deduced by electron diffraction. The first study was made with the gas phase, but the author did not place much reliance on his results owing to the instability of his sample.[4] The second investigation was made in a solution of benzene; this led to a value of 0.50 D.[5] However, a recent unsuccessful search for microwave absorption in the gas phase places an upper limit at 0.1 D for this molecule.[6]

(1) A. Stock and R. Wierl, *Z. Anorg. Allgem. Chem.*, **203**, 228 (1932).

(2) S. H. Bauer, *J. Am. Chem. Soc.*, **60**, 524 (1938).

(3) E. W. Hughes, *ibid.*, **78**, 502 (1956).

(4) K. L. Ramaswamy, *Proc. Indian Acad. Sci.*, **A2**, 364, 630 (1935).

(5) H. Watanabe and M. Kubo, *J. Am. Chem. Soc.*, **82**, 2428 (1960).

(6) C. C. Costain, private communication, National Research Council of Canada.

All the spectra of borazine have been interpreted on the assumption that its symmetry is D_{3h}. The ultraviolet spectrum[7] was accounted for by self-consistent field, molecular orbital calculations, assuming that a pair of electrons on each nitrogen atom is available for bonding in the π system.[8] More recent Hückel MO calculations for borazine and the B-trihalogneated derivatives show a direct correlation between the calculated electron densities on the ring atoms and the chemical shifts observed in the ^{11}B and ^{14}N nuclear magnetic resonance spectra.[9] However, extended Hückel MO calculations and other MO calculations[10-12] indicate that although some electron density is shifted from N to B in the π system, the σ bond is polarized in the *opposite* direction making the nitrogens negative with respect to the borons. The magnitudes of the calculated electron density shifts depend on the details of the analyses, but all of these suggest that the principal stabilization in the ring system results from polar σ bonds with additional bonding in the p–π system.

The infrared spectra of B-trifluoroborazine, trifluoro-*s*-triazine, and 1,3,5-trifluorobenzene show a progressive increase in the ring-stretching frequency.[13] This is consistent with the assumption that borazine is less aromatic than *s*-triazine or benzene. The magnitude of the diamagnetic anisotropy also indicates that in borazine there is less electron delocalization than in benzene.[14,15]

Experimental Section

A sample of borazine was prepared by the reaction of $LiBH_4$ and NH_4Cl. The $B_2H_5NH_2$ impurity was removed by addition of excess ammonia to precipitate the nonvolatile adduct. The unreacted ammonia was then removed by pumping on the residue, condensed at −78°. In a purified sample of borazine at 50 mm pressure, no NH_3 could be detected by infrared absorption in a 10-cm cell. This established an upper limit of 1% for any ammonia remaining in the sample.

Sectored electron diffraction photographs were taken in the convergent mode with the new Cornell apparatus.[16] During exposures the sample was maintained at −40°. The diffraction patterns from a 70-kV electron beam were recorded on 4 × 5 in. Kodak Process plates. The nozzle was placed approximately at 126 mm and at 254 mm from the photographic plates; useful diffraction patterns were thus obtained over the region q = 8–125. Two sets of plates, of samples individually synthesized, tested for purity and photographed at an interval of 4 months, were analyzed separately.

The diffraction patterns were read as pen recorder tracings of photographic density obtained with a Jarrell-Ash microphotometer, interfaced with a Bristol recorder. In addition, the patterns were converted to digitized optical densities using the same microphotometer interfaced with a digital voltmeter.[17] These two methods of transcribing the diffraction patterns were compared by analyzing the four sets of data separately. Because the first analysis, when completed, led to a nonplanar conformation, a conclusion we found difficult to accept, we considered it worthwhile to repeat the experiment in its entirety and to devote so large an effort to this investigation in order to reduce as much as possible effects resulting from consistent errors of which we may be unaware.

The plate–nozzle distance and the wavelength of the incident electrons were determined by calibration, using MgO powder photographs recorded with each sample. Since the short and long sample–plate distances were obtained by rotating an off-set injection tube

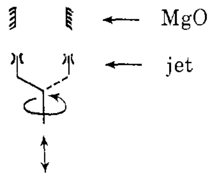

with the MgO sample fixed directly over the gas exit hole, misalignment of the reference sample, if present, would have introduced a discrepancy between the $q_{\max}$ positions for the regions over which the two sets of patterns overlapped. This was not observed. The optical densities were converted to scattered intensities by a method described elsewhere.[18] The data were also corrected for the flatness of the photographic plates. The diffraction intensities are listed in Table I.

The reduction of the diffraction intensity data to obtain molecular parameters followed the conventional analysis. The molecular intensity function, $(\pi/10)qM(q)$, and radial distribution function, $f(r)$, were calculated as outlined by Bonham and Bartell.[19] The distribution curves were calculated with a damping factor $\gamma = 0.00149$, chosen so that $\pi^2\gamma q_{\max}^2/100 = 0.1$. After refinement of the experimental background, the structural parameters were evaluated by fitting the experimental molecular intensity curve, $P(q)\pi/10qM(q)$, by least-squares analysis.[20] The weighting function, $P(q)$, used in that analysis was $P(q) = \exp[-w_1(20 - q)]$ for $q < 20$ and w_1 such that $P(q) = 0.25$ at $q = 8$; $P(q) = 1.00$ for $20 < q < 105$; $P(q) = \exp[-w_2(q - 105)]$ for $q > 105$ and w_2 such that $P(q) = 0.1$ at $q = 125$. The atom form factors of Cromer, Larson, and Waber[21] and the phase shift factors of Bonham and Ukaji[22] were used in the analysis.

Structural Deductions

As stated above, diffraction patterns of two different samples were obtained and the photographs were analyzed from recorder tracings and from digital voltmeter prints-outs of the density *vs.* pattern radius. Each of these sets of data was carried through the complete analysis, on an individual basis, and fitted by least squares. The recorder data showed slightly lower standard deviations for the final fit for all models and for both samples. This *apparent* better fit is presumed to be a consequence of correlation in the diffraction data due to motion (during the recording) of the carriage in which the rotating plate is mounted, to damping in the recorder, and to subjective smoothing of the data in reading the recorder traces. Modifications of the microphotometer, which incorporated a precision drive screw and a digitizing unit, greatly reduced these correlations. The digital voltmeter gives up to five significant figures with

---

(7) C. W. Rector, G. W. Schaeffer, and J. R. Platt, *J. Chem. Phys.*, **17**, 460 (1949).

(8) D. W. Davies, *Trans. Faraday Soc.*, **56**, 1713 (1960).

(9) K. Hansen and K. P. Messer, *Theoret. Chim. Acta*, **9**, 17 (1967).

(10) R. Hoffman, *J. Chem. Phys.*, **40**, 2474 (1964).

(11) O. Chalvet, R. Daudel, and J. J. Kaufman, *J. Am. Chem. Soc.*, **87**, 399 (1965).

(12) P. M. Kuznesof and D. F. Shriver, *ibid.*, **90**, 1683 (1968).

(13) H. Beyer, H. Jenne, J. B. Hynes, and K. Niedenzu, Advances in Chemistry Series, No. 42, American Chemical Society, Washington, D. C., 1964, p 266.

(14) K. Lonsdale, *Nature*, **184**, Suppl. 4, 1060 (1959).

(15) H. Watanabe, K. Ito, and M. Kubo, *J. Am. Chem. Soc.*, **82**, 3294 (1960).

(16) S. H. Bauer, "Electron Diffraction Studies at High Temperatures," Nonr-401(41), Project NR092-504, ARPA Order No. 23-53, Dec 1967.

(17) S. H. Bauer, R. L. Hilderbrandt, and R. Jenkins, to be submitted for publication.

(18) J. L. Hencher and S. H. Bauer, *J. Am. Chem. Soc.*, **89**, 5527 (1967).

(19) R. A. Bonham and L. S. Bartell, *J. Chem. Phys.*, **31**, 702 (1959); see also J. L. Hencher and S. H. Bauer, *J. Am. Chem. Soc.*, **89**, 5529 (1967).

(20) K. Hedberg and M. Iwasaki, *Acta Cryst.*, **17**, 529 (1964).

(21) D. T. Cromer, A. C. Larson, and J. T. Waber, Report LA-2987, Los Alamos Scientific Laboratory, Los Alamos, N. M., 1963.

(22) R. A. Bonham and T. Ukaji *J. Chem. Phys.*, **36**, 72 (1962).

TABLE I[a]

DIFFRACTION DATA FOR BORAZINE

Set 1
Long Sample-plate
Distance

Q	INTENSITY
8.	1.0018
9.	0.8698
10.	0.7321
11.	0.6272
12.	0.5496
13.	0.5299
14.	0.5928
15.	0.7335
16.	0.9293
17.	1.0917
18.	1.1499
19.	1.0905
20.	0.9604
21.	0.8226
22.	0.7258
23.	0.6853
24.	0.6958
25.	0.7377
26.	0.7862
27.	0.8320
28.	0.8710
29.	0.9014
30.	0.9203
31.	0.9291
32.	0.9333
33.	0.9347
34.	0.9314
35.	0.9169
36.	0.8801
37.	0.8332
38.	0.7955
39.	0.7921
40.	0.8297
41.	0.9014
42.	0.9814
43.	1.0365
44.	1.0502
45.	1.0296
46.	0.9987
47.	0.9827
48.	0.9850
49.	0.9989
50.	1.0056
51.	0.9952
52.	0.9757
53.	0.9604
54.	0.9665
55.	0.9986
56.	1.0524
57.	1.1089
58.	1.1517
59.	1.1657
60.	1.1595
61.	1.1462
62.	1.1319
63.	1.1282
64.	1.1348
65.	1.1471
66.	1.1646
67.	1.1782
68.	1.1923
69.	1.1980
70.	1.1803
71.	1.0907
72.	0.6359

Short Sample-plate
Distance

Q	INTENSITY
26.	0.5382
27.	0.5404
28.	0.5418
29.	0.5312
30.	0.5194
31.	0.5033
32.	0.4869
33.	0.4742
34.	0.4639
35.	0.4484
36.	0.4256
37.	0.3953
38.	0.3682
39.	0.3660
40.	0.3881
41.	0.4191
42.	0.4522
43.	0.4727
44.	0.4697
45.	0.4572
46.	0.4404
47.	0.4310
48.	0.4298
49.	0.4350
50.	0.4348
51.	0.4272
52.	0.4161
53.	0.4061
54.	0.4104
55.	0.4244
56.	0.4493
57.	0.4754
58.	0.4903
59.	0.4969
60.	0.4899
61.	0.4808
62.	0.4722
63.	0.4661
64.	0.4693
65.	0.4730
66.	0.4772
67.	0.4822
68.	0.4870
69.	0.4926
70.	0.5030
71.	0.5144
72.	0.5261
73.	0.5322
74.	0.5379
75.	0.5375
76.	0.5331
77.	0.5294
78.	0.5293
79.	0.5284
80.	0.5329
81.	0.5418
82.	0.5508
83.	0.5646
84.	0.5767
85.	0.5874
86.	0.5946
87.	0.5998
88.	0.6038
89.	0.6062
90.	0.6122
91.	0.6180
92.	0.6225
93.	0.6261
94.	0.6308
95.	0.6410
96.	0.6521
97.	0.6654
98.	0.6795
99.	0.6944
100.	0.7031
101.	0.7122
102.	0.7201
103.	0.7261
104.	0.7339
105.	0.7405
106.	0.7488
107.	0.7609
108.	0.7712
109.	0.7826
110.	0.7946
111.	0.8087
112.	0.8227
113.	0.8366
114.	0.8521
115.	0.8668
116.	0.8770
117.	0.8884
118.	0.9007
119.	0.9145
120.	0.9266
121.	0.9417
122.	0.9592
123.	0.9744
124.	0.9890
125.	1.0066
126.	1.0198
127.	1.0319
128.	1.0473
129.	1.0551
130.	1.0634
131.	1.0664
132.	1.0681
133.	1.0636
134.	1.0534
135.	1.0388
136.	1.0132
137.	0.9755
138.	0.9235
139.	0.8580
140.	0.7868
141.	0.6971
142.	0.4354

Set 2
Long Sample-plate
Distance

Q	INTENSITY
8.	2.2405
9.	1.9098
10.	1.6140
11.	1.4164
12.	1.2328
13.	1.2055
14.	1.3419
15.	1.6422
16.	2.0264
17.	2.3400
18.	2.4449
19.	2.3333
20.	2.0857
21.	1.8167
22.	1.6166
23.	1.5344
24.	1.5563
25.	1.6410
26.	1.7448
27.	1.8341
28.	1.9124
29.	1.9711
30.	2.0090
31.	2.0283
32.	2.0332
33.	2.0373
34.	2.0316
35.	2.0071
36.	1.9373
37.	1.8393
38.	1.7550
39.	1.7374
40.	1.8076
41.	1.9472
42.	2.1047
43.	2.2178
44.	2.2422
45.	2.2036
46.	2.1409
47.	2.1020
48.	2.1021
49.	2.1256
50.	2.1393
51.	2.1194
52.	2.0808
53.	2.0448
54.	2.0501
55.	2.1107
56.	2.2090
57.	2.3158
58.	2.4005
59.	2.4388
60.	2.4320
61	2.4012
62.	2.3720
63.	2.3544
64.	2.3689
65.	2.3903
66.	2.4193
67.	2.4480
68.	2.4734
69.	2.4836
70.	2.4517
71.	2.3060
72.	1.3321

Short Sample-plate
Distance

Q	INTENSITY
26.	0.9169
27.	0.9370
28.	0.9316
29.	0.9160
30.	0.8929
31.	0.8643
32.	0.8360
33.	0.8120
34.	0.7906
35.	0.7629
36.	0.6817
37.	0.6595
38.	0.6182
39.	0.6082
40.	0.6375
41.	0.6893
42.	0.7442
43.	0.7735
44.	0.7754
45.	0.7524
46.	0.7255
47.	0.7089
48.	0.7047
49.	0.7146
50.	0.7135
51.	0.6988
52.	0.6784
53.	0.6591
54.	0.6646
55.	0.6882
56.	0.7275
57.	0.7669
58.	0.7934
59.	0.7996
60.	0.7903
61.	0.7719
62.	0.7577
63.	0.7495
64.	0.7504
65.	0.7555
66.	0.7619
67.	0.7682
68.	0.7763
69.	0.7853
70.	0.7993
71.	0.8152
72.	0.8316
73.	0.8440
74.	0.8503
75.	0.8490
76.	0.8437
77.	0.8368
78.	0.8311
79.	0.8296
80.	0.8337
81.	0.8449
82.	0.8588
83.	0.8750
84.	0.8925
85.	0.9055
86.	0.9139
87.	0.9203
88.	0.9228
89.	0.9286
90.	0.9309
91.	0.9336
92.	0.9359
93.	0.9378
94.	0.9425
95.	0.9514
96.	0.9652
97.	0.9824
98.	1.0011
99.	1.0163
100.	1.0286
101.	1.0369
102.	1.0417
103.	1.0466
104.	1.0548
105.	1.0623
106.	1.0711
107.	1.0789
108.	1.0896
109.	1.1020
110.	1.1140
111.	1.1280
112.	1.1444
113.	1.1611
114.	1.1761
115.	1.1885
116.	1.1999
117.	1.2093
118.	1.2207
119.	1.2295
120.	1.2391
121.	1.2519
122.	1.2647
123.	1.2763
124.	1.2915
125.	1.3084
126.	1.3177
127.	1.3317
128.	1.3408
129.	1.3476
130.	1.3573
131.	1.3628
132.	1.3645
133.	1.3595
134.	1.3503
135.	1.3336
136.	1.3084
137.	1.2673
138.	1.2088
139.	1.1345
140.	1.0546
141.	0.9812
142.	0.6826

[a] For density–intensity conversion see ref 18. The *Q* scale was obtained by interpolation, using three times as many points as are listed. Plate position readings are reproducible to ±5 μ.

a noise level of less than 5 parts in 10,000. Transmittance readings were taken with the plate rotating but not translating. Points were read at 3-sec intervals to allow for adequate averaging for the response time of the digitizing unit. In addition, transmittance readings were recorded at intervals of $q/3$. Optical density readings were then obtained at integral values of q by a six-point Lagrangian interpolation program. Molecular intensity calculations were made with data at integral values of q in conformance with the findings of Murata and Morino.[23] This procedure for data analysis effectively reduced the correlation in intensity readings at adjacent values of q to less than $|\pm 0.15|$.

Comparison of the results of the digitized and recorder data indicated that the converged solutions for data set 2 agreed within the uncertainty of the parameters for nearly all parameters of all models tested. For data set 1 the difference was slightly outside the uncertainties. Only the digitized data for the two samples are given in Table I.

Table II lists the converged structural parameters for the two samples analyzed and for the three models tested. The listed uncertainties are those derived from the least-squares fit of the reduced intensity values. In Figure 1 the observed intensity curves are traced, and the background is drawn in for the two samples. Figure 2 is a compilation of the experimental molecular intensity curves for the two samples and the fitted curves for the three models. The experimental radial distribution curves are shown in Figure 3.

Three conformations with different molecular symmetries were used as models in the least-squares analysis of the data: planar, with D_{3h} symmetry; a chair model, C_{3v} symmetry; a twisted model, C_2 symmetry. Two C_s models—a chair form and a boat form—each with two equivalent B and two equivalent N atoms may also be considered. In view of our experience with the C_{3v} and C_2 models there is no doubt that C_s conformations can be found which will fit the intensity data equally well. However, since a slight adjustment of parameters will convert the C_s chair and boat forms into the C_{3v} and C_2 structures, respectively, these C_s models were not analyzed in detail.

In Table II, σ is the standard deviation of the least-squares fit as given by the formula[24]

$$\sigma = \sqrt{\frac{\chi^2}{n - m}}$$

where χ^2 is the weighted sum of the squares of the deviations, given in Table I, n is the number of data points used (*i.e.*, one-third of the number of points recorded), and m is the number of parameters. The dispersion of σ may be calculated from the formula[25] $\Delta\sigma = \sigma/[2(n - m)]^{1/2}$.

---

(23) Y. Murata and Y. Morino, *Acta Cryst.*, **20**, 605 (1966).

(24) N. Arley and K. R. Buch, "Introduction to the Theory of Probability and Statistics," John Wiley & Sons, Inc., New York, N. Y., 1950, p 188.

(25) See ref 24, p 191.

Table II

Least-Squares Structural Parameters for Borazine

	D_{3h}		C_{3v}		C_2	
Parameter[a]	Set 1	Set 2	Set 1	Set 2	Set 1	Set 2
B–N	1.4343 ± 0.0006	1.4336 ± 0.0005	1.4352 ± 0.0005	1.4350 ± 0.0004	1.4356 ± 0.0005	1.4349 ± 0.0005
B–H	1.2475 ± 0.0071	1.2395 ± 0.0077	1.2514 ± 0.0062	1.2587 ± 0.0070	1.2559 ± 0.0043	1.2577 ± 0.0048
N–H	1.0482 ± 0.0058	1.0358 ± 0.0056	1.0602 ± 0.0051	1.0484 ± 0.0048	1.0637 ± 0.0038	1.0478 ± 0.0038
N···N					2.4642 ± 0.0031	2.4568 ± 0.0026
B···B					2.4961 ± 0.0042	2.5022 ± 0.0036
∠NBN	117.13 ± 0.26	117.21 ± 0.21	119.47 ± 0.4	118.69 ± 0.4	117.9 ± 0.4	117.5 ± 0.4
∠ring out of plane			13.3 ± 1.1	13.2 ± 1.0		
NH out of plane			−35.8 ± 2.2	−31.9 ± 2.3	42.3 ± 1.7	36.7 ± 2.3
∠BH out of plane			23.2 ± 3.1	27.0 ± 2.6	42.3 ± 1.7	36.7 ± 2.3
l_{B-N}	0.0589 ± 0.0013	0.0573 ± 0.0010	0.0575 ± 0.0010	0.0554 ± 0.0008	0.0570 ± 0.0003	0.0562 ± 0.0009
l_{B-H}	0.0525 ± 0.0051	0.0651 ± 0.0062	0.0537 ± 0.0043	0.0644 ± 0.0045	0.0547 ± 0.0037	0.0630 ± 0.0039
l_{N-H}	0.0736 ± 0.0046	0.0784 ± 0.0048	0.0749 ± 0.0036	0.0814 ± 0.0035	0.0757 ± 0.0032	0.0803 ± 0.0031
$l_{BB} = l_{NN}$	0.0711 ± 0.0022	0.0670 ± 0.0020	0.0766 ± 0.0017	0.0743 ± 0.0009	0.0752 ± 0.0009	0.0719 ± 0.0011
$l_{N...B}$	0.0739 ± 0.0025	0.0724 ± 0.0022	0.0733 ± 0.0019	0.0718 ± 0.0016	0.0724 ± 0.0015	0.0718 ± 0.0014
σ	0.03369	0.02938	0.02415	0.01978	0.02095	0.01978
$\Delta\sigma$	0.0023	0.0020	0.00024	0.0019	0.0020	0.0019
Errors	0.121480	0.092350	0.060672	0.040691	0.045639	0.040686

[a] Distances are in ångströms and angles are in degrees.

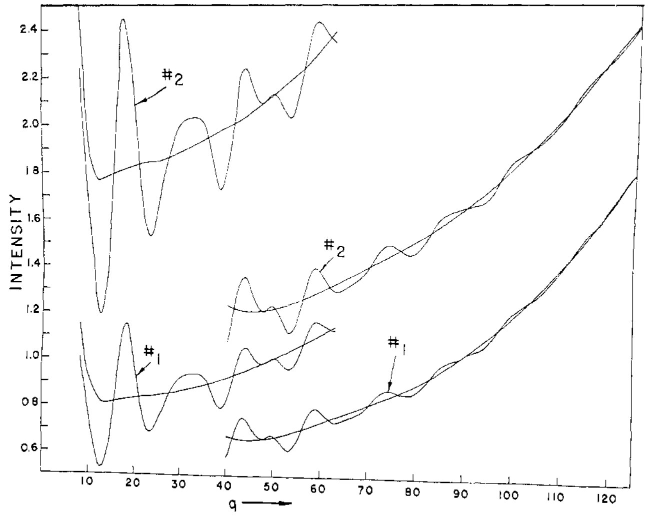

Figure 1.—The observed scattered intensity as a function of angle [$q \equiv (4\pi/\lambda)(\sin\theta)/2$] for the two samples of borazine.

Comparison of the σ's for the best models from Table II indicates that both of the nonplanar structures fit the experimental data significantly better than does the planar D_{3h} conformation. Using the *t* distribution for the test of significance of the least-squares fit,[26] the following conclusions are apparent: (a) for a given model the two sets of data agree within the 95% confidence interval; (b) the two nonplanar models are indistinguishable within the 95% confidence interval; (c) the σ for the planar D_{3h} model for either set of data is beyond the 99% confidence interval of the σ for either nonplanar model. In other words, the two sets of data are separately fitted better by the nonplanar models which are statistically distinguishable from the planar model.

Of the two nonplanar models the C_{3v} model may be discarded as inconsistent with a microwave investigation of borazine. Estimates based on electron densities from MO calculations[12] and the geometry of the C_{3v} model lead to an expected dipole moment of approximately 0.3 D. This is inconsistent with the absence of a measurable microwave absorption by gaseous borazine;[6] the basis for discarding the C_s chair model is even stronger. Hence the choice reduces to either a model possessing C_2 symmetry with amplitudes for intramolecular motion which are comparable to those found in many other similar ring compounds or to the assumption that borazine has D_{3h} symmetry with excessively large distortions from planarity due to perpendicular

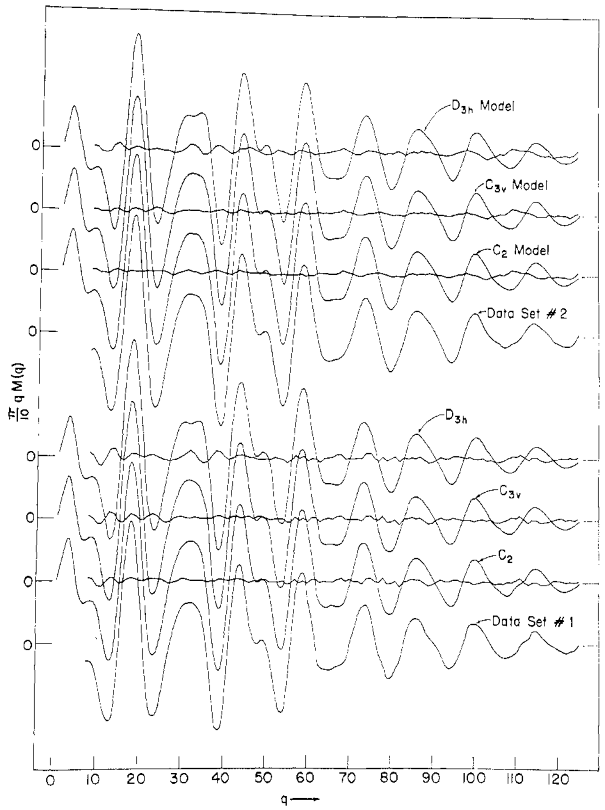

Figure 2.—Comparison of calculated with observed intensity patterns for the best parameters deduced by least squares for the three models considered in detail. The jagged curves show the deviations between the calculated and observed values.

---

(26) See ref 24, p 97.

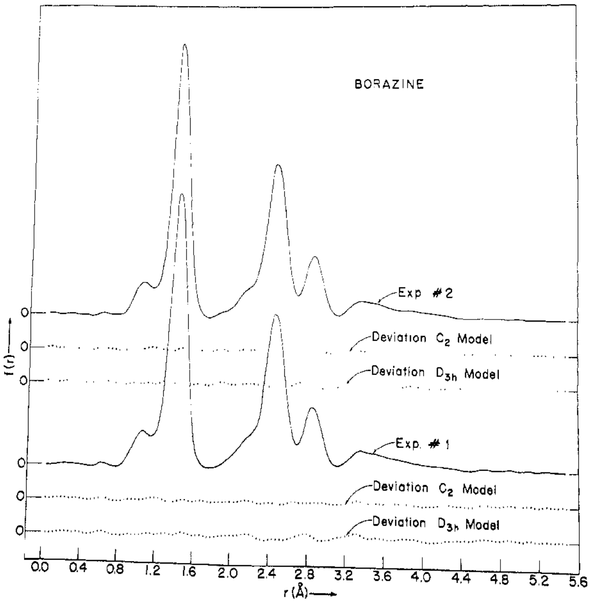

Figure 3.—The refined radial distribution curves for borazine.

type vibrational motions. The fitted parameters for the C_2 model are listed in Table III.

TABLE III

C_2 MODEL FOR BORAZINE

Interatomic Distances (r_a), Å

B–N	1.4355 ± 0.0021
B–H	1.258 ± 0.014
N–H	1.050 ± 0.012
N···N	2.460 ± 0.009
B···B	2.499 ± 0.012

Angles, Deg

∠NBN	117.7 ± 1.2
∠BNB	121.1 ± 1.2
∠NH out of plane ∠BH out of plane	39.5 ± 6

Amplitudes of Vibration, Å

B–N	0.057 ± 0.002
B–H	0.059 ± 0.012
N–H	0.078 ± 0.009
B···B N···N	0.074 ± 0.003
N···B	0.072 ± 0.003

The estimation of random errors in electron diffraction analysis has been outlined by Morino, Kuchitsu, and Murata[27] in their study of the least-squares procedure of analysis. Sources of error are calibration of the electron wavelength, plate to nozzle distance, imperfections in the sector shape, sample spread, uncertainties in elastic and inelastic scattering factors, and effects of anharmonicity. One estimate of the errors of the data is obtained from the uncertainties for the parameters given by the least-squares fit. These are listed in Table II. A second estimate of the random errors is obtained from a comparison of the two sets of data obtained independently. With the exception of the uncertain N–H bond length, the two sets of data are consistent within three times the standard deviations of the least-squares fit.

Of the systematic errors listed above, the largest uncertainty arises from the calibration of the wavelength and plate to nozzle distance. This calibration was made by fitting by a steepest descents analysis the measured to calculated positions of several rings of an MgO powder pattern to obtain the most consistent values for the wavelength and plate to nozzle distance for each set of data. This analysis led to an uncertainty in q of ±0.0012 in establishing the q scale. Such an uncertainty introduces a corresponding uncertainty of ±0.002 Å in the B–N bond length. The error limits listed in Table III are, thus, ±0.002 Å for the bond lengths or three times the standard deviations from the least-squares analysis, whichever is larger. The least-squares analysis showed no large correlations between parameters.

From Table II it appears that all of the bonded distances are larger for the nonplanar structures than for the planar model. This indicates that the constraint of planarity on the model forces a compromise fit of the complete pattern. More explicitly, for a given set of structural parameters the nonbonded distances are maximized in the planar structure; therefore, if a planar model is used to fit a pattern produced by a nonplanar structure, the bonded distances must be shortened to accommodate the nonbonded distances.

Using the assigned N–H and B–N stretching frequencies, 3452 and 2535 cm^{-1}, respectively, from the infrared spectrum of borazine[28] the amplitudes of vibration were calculated for these two atom pairs. The A_1' normal vibrations of borazine are well separated into two high-frequency modes and two of lower frequency. If the force constants for the lower frequencies are set equal to zero, a good approximation to the force constants for the N–H and B–H stretching frequencies may be estimated.[29] From this the amplitudes of vibration were calculated to be 0.0723 Å for N–H and 0.0855 Å for B–H. Comparison with the values listed in Table II shows that the calculated N–H amplitude agrees reasonably well with the experimental value. The observed B–H amplitude is more uncertain, as is apparent from the radial distribution curves shown in Figure 3; the B–H bonded distance appears only as a shoulder to the left of the large B–N peaks. This uncertainty is reflected in the discrepancy between the observed and estimated B–H amplitudes of vibration.

To ascertain if vibrational motion of the molecule can account for the observed nonplanarity, the shrinkage effect for the nonbonded B–H distance was calculated for the two nonplanar models. For this molecule the shrinkage across the ring is the difference between the *observed* nonbonded B–N distance and a *value calculated,* using the observed B–N bonded distance of the nonplanar model and the observed N–N nonbonded distance of the nonplanar model, on the assumption that

---

[27] Y. Morino, K. Kuchitsu, and Y. Murata, *Acta Cryst.*, **18**, 549 (1965).

[28] K. Niedenzu, W. Sawodny, H. Watanabe, J. W. Dawson, T. Totani, and W. Weber, *Inorg. Chem.*, **6**, 1453 (1967).

[29] E. B. Wilson, Jr., J. C. Decius, and P. C. Cross, "Molecular Vibrations," McGraw-Hill Book Co., Inc., New York, N. Y., 1955.

the sum of the adjacent ∠BNB and ∠NBN bond angles in the ring is 240°. The natural shrinkage[30] was calculated after the observed internuclear distances were adjusted to r^g values[31]

$$-\delta = (r^g{}_{B\cdots N})_{obsd} - [(r^g{}_{B-N})^2 + (r^g{}_{N\cdots N})^2 - 2(r^g{}_{B-N})(r^g{}_{N\cdots N}) \cos \alpha]$$

where α is the angle between $r_{N\cdots N}$ and r_{B-N} determined such that the sum of adjacent ∠BNB and ∠NBN bond angles is 240°.

The results are listed in Table IV. These values are exceptionally large for such shrinkage effects, in comparison with the shrinkage calculated for the *para* distance in benzene, on the basis of its spectroscopic parameters,[32] also shown in Table IV.

TABLE IV

SHRINKAGE EFFECTS ($-\delta$, Å)[a]

C_{3v}		C_2	
Set 1	Set 2	Set 1	Set 2
0.017	0.017	0.010	0.007
		0.026	0.021

[a] Owing to its lower symmetry the C_2 model has two different B···N (nonbonded) distances. Benzene shrinkage (*para* distance)[32] is 0.00485 Å.

Cartesian coordinates for the converged structures with D_{3h} and C_2 symmetries, for the second set of data, are listed in Table Va and b, respectively. The nonplanarity of the C_2 model as measured by the z coordinates is typical of the magnitudes observed in all converged nonplanar models.

TABLE V

a. CARTESIAN COORDINATES OF D_{3h} MODEL (Å) (ALL Z COORDINATES ARE ZERO)

Atom	X	Y
B(1)	0.0	1.4540
N(2)	1.2240	0.7069
B(3)	1.2592	−0.7270
N(4)	0.0	−1.4134
B(5)	−1.2592	−0.7270
N(6)	−1.2240	0.7069
H(1)	2.1304	1.2300
H(2)	2.3365	−1.3490
H(3)	0.0	−2.4600
H(4)	−2.3365	−1.3490
H(5)	−2.1304	1.2300
H(6)	0.0	2.6980

b. Cartesian Coordinates of C_2 Model (Å)

Atom	X	Y	Z
B(1)	0.0	1.4447	0.0
N(2)	1.2238	0.7031	0.1065
B(3)	1.2465	−0.7158	−0.1065
N(4)	0.0	−1.4185	0.0
B(5)	−1.2465	−0.7158	0.1065
N(6)	−1.2238	0.7031	−0.1065
H(1)	0.0	2.7023	0.0
H(2)	1.9510	1.1229	0.7332
H(3)	2.1194	−1.2197	−0.8588
H(4)	0.0	−2.4663	0.0
H(5)	−2.1194	−1.2197	0.8588
H(6)	−1.9310	1.1229	−0.7332

Discussion

The boron–nitrogen bond length of 1.4355 ± 0.002_1 Å is in good agreement with the previously determined value of 1.44 ± 0.02 Å[2] and is comparable with the reported bond lengths of 1.42 Å in N-trimethylborazine, 1.41 Å in B-trichloroborazine,[33] 1.426 Å in B-trifluoroborazine,[34] and 1.429 Å for the ring B–N distance in B-monoaminoborazine.[35] The B–H bond length of 1.259 ± 0.019 Å is somewhat longer than values reported for other compounds. In N-trimethylborazine the corresponding bond length is 1.20 Å,[33] close to that found in boroxine, $B_3O_3H_3$ (1.192 Å).[36] However, this difference correlates well with the corresponding magnitudes of the stretching frequencies. The symmetric and asymmetric frequencies for B–H in borazine are 2535 and 2520 cm^{-1}, respectively,[28] while they are 2616 and 2613 cm^{-1} in boroxine.[37]

An interesting result of this structure analysis is that the ∠NBN bond angle is 117° while ∠BNB is greater than 120°, by an amount which depends on the degree of planarity of the ring. (Parenthetically, the least-squares analysis clearly resolved this assignment. In one test an approximate structure was inserted in which ∠NBN = 123° and ∠BNB = 117° were assumed. In rapid succession the sequence of cycles converged to the quoted values, showing that the atom form factors for B and N differ sufficiently for distinction by the least-squares calculation.) In the crystal structure of B-trichloroborazine ∠NBN was found to be 119°[38] and the same value was obtained in the electron diffraction study of B-trifluoroborazine,[33] both compounds with D_{3h} symmetry. In boroxine ∠OBO is 120°[36] and the molecule is planar, while in *s*-triazine ∠CNC is 113°[39] and the molecule is planar.

The magnitudes of the ∠BNB and ∠NBN angles in borazine and the substituted borazines, as compared to ∠CNC in *s*-triazine, may be qualitatively rationalized, as follows. MO calculations that involve more atomic orbitals than the p–π system indicate that in borazine, 0.48 electron is transferred from a nitrogen to a boron atom in the p–π system. However, the σ bond is so strongly polarized in the opposite direction that each nitrogen atom assumes a net negative charge of −0.231, and the net positive charge on each boron atom is +0.322.[12] Qualitatively, this indicates that there is more p character in the boron hybridization than in a trigonal sp^2 hybrid, leading to a ring ∠NBN of less than 120°; the corresponding increase in s character for the hybridization on the nitrogen makes ∠BNB greater than 120°. In the isoelectronic *s*-triazine, where the

---

[30] Y. Morino, S. J. Cyvin, K. Kuchitsu, and T. Iijima, *J. Chem. Phys.*, **36**, 1109 (1962).

[31] U. Morino, Y. Nakamura, and T. Iijima, *ibid.*, **32**, 643 (1960).

[32] W. V. F. Brooks, B. N. Cyvin, S. J. Cyvin, P. C. Kvande, and E. Meisingseth, *Acta Chem. Scand.*, **17**, 345 (1963).

[33] K. P. Coffin and S. H. Bauer, *J. Phys. Chem.*, **59**, 193 (1955).

[34] S. H. Bauer, K. Katada, and K. Kimura, "Structural Chemistry and Molecular Biology," A. Rich and N. Davidson, Ed., W. H. Freeman and Co., San Francisco, Calif., 1968, p 653.

[35] W. Harshbarger, G. Lee, R. F. Porter, and S. H. Bauer, *J. Am. Chem. Soc.*, **91**, 551 (1969).

[36] C. H. Chang, R. F. Porter, and S. H. Bauer, *Inorg. Chem.*, **8**, 1689 (1969).

[37] F. A. Grimm, L. Barton, and R. F. Porter, *ibid.*, **7**, 1309 (1968).

[38] D. L. Coursen and J. L. Hoard, *J. Am. Chem. Soc.*, **74**, 1742 (1952).

[39] J. E. Lancaster and B. P. Stoicheff, *Can. J. Phys.*, **34**, 1016 (1956).

∠CNC is 113°, the conclusion is that, owing to their greater electronegativity, the nitrogens localize the p–π electrons, decreasing the aromatic character of the molecule.

A major point of interest in this analysis of the structure of borazine is the degree of nonplanarity of the molecule. As stated above, both nonplanar models fit the experimental data significantly better than does a rigid D_{3h} model. In Figure 2 it is seen that in the region q = 30–35 the planar model exhibits a slight splitting at the maximum that is not present in either set of experimental data nor in either of the nonplanar models. The resolutions of the electron diffraction photographs and of the microphotometer system are sufficient to show such a feature in the experimental data if it were present.

The calculated shrinkage effect for the two nonplanar models is unusually large. The values obtained are two to four times the comparable value calculated for benzene, as shown in Table IV, and ten times the least-squares standard deviation for N···N. The magnitude of the shrinkage effects leads to the question of whether the observed nonplanarity of the best fitting models is a result of large oscillatory distortions due to vibrational motion.

The choice, then, for the best way to describe the molecular structure of borazine is between a planar D_{3h} model, with exceptionally large out-of-plane vibrational motions such that the probability distribution approaches that for a classical oscillator, and a C_2 model, which is nonpolar in its lowest energy configuration. This choice is not unambiguous, and at this stage, a decision rests on personal preferences. Ultimately the question reduces to one of determining the shape of the potential function of the molecule for out-of-plane distortions. This might be accomplished by a detailed study of the effect of reduced sample temperature on the diffraction patterns. The lowest assigned frequency for borazine (based on D_{3h} symmetry) is 288 cm^{-1}, and the next lowest vibrational frequency is an out-of-plane vibration at 394 cm^{-1}.[28] These correspond to an E_{2u} vibration in benzene, at 404 cm^{-1}, and a B_{2g} vibration at 530 cm^{-1}, indicating considerably lower force constants for distortion from planarity in borazine.

Kubo and his coworkers have calculated simple valence force constants for borazine.[40] However, the recent extensive study of the infrared and Raman spectra[28] of borazine would alter the values of these force constants. A complete normal-coordinate analysis of borazine is expected based on the more recent assignment. It is beyond the scope of this paper to make this normal-coordinate analysis. However, such an analysis must account for the observed nonplanarity of borazine either by assigning a symmetry lower than D_{3h} for the molecule or by indicating the nature of the vibrational motion which results in the observed large shrinkage effects.

Acknowledgments.—This work was supported by the Advanced Research Projects Agency, Army Research Office (Durham), and the National Science Foundation.

(40) H. Watanabe, M. Narisada, T. Nakagawa, and M. Kubo, *Spectrochim. Acta*, **16**, 78 (1960).

CONTRIBUTION FROM THE DEPARTMENT OF CHEMISTRY,
CORNELL UNIVERSITY, ITHACA, NEW YORK. 14850

The Molecular Structure of Boroxine, $H_3B_3O_3$, Determined by Electron Diffraction[1]

BY C. H. CHANG, R. F. PORTER, AND S. H. BAUER

Received January 8, 1969

The structure of $H_3B_3O_3$ in the gas phase has been determined by electron diffraction, using digitized microdensitometric data. The heavy atoms are arranged in a planar six-membered ring (D_{3h}). Several nonplanar structures were considered and limits were set on the magnitude of out-of-plane distortion for the average conformation. The bond lengths are B–H = 1.192 ± 0.017 and B–O = $1.375_8 \pm 0.002_1$ Å. The bond angles are 120 ± 0.64°.

Introduction

The chemical behavior of boroxine ($H_3B_3O_3$) has been discussed in a series of recent publications.[2,3] The gaseous compound was first observed as one of the products of a high-temperature reaction of H_2 with B–B_2O_3 mixtures.[4] It is also a product in the explosive oxidation of B_2H_6[2] and of B_5H_9.[5] At ambient temperatures, $H_3B_3O_3$ is thermally unstable and decomposes to B_2H_6 and B_2O_3. It has generally been assumed that boroxine is a six-membered heterocyclic ring, similar in structure to borazine ($B_3N_3H_6$). Infrared spectral data may be readily interpreted on the basis of a ring structure.[6]

Since $H_3B_3O_3$ is the simplest member of a large family of boroxine derivatives, it is of importance to define its structure quantitatively. In this paper, we report on

---

(1) Work supported by the Army Research Office (Durham) and the Advanced Research Projects Agency.

(2) L. Barton, F. A. Grimm, and R. F. Porter, *Inorg. Chem.*, **5**, 2076 (1966).

(3) G. H. Lee, II, and R. F. Porter, *ibid.*, **5**, 1329 (1966).

(4) W. D. Sholette and R. F. Porter, *J. Phys. Chem.*, **67**, 177 (1963).

(5) G. H. Lee, II, W. H. Bauer, and S. E. Wiberley, *ibid.*, **67**, 1742 (1963).

(6) S. K. Wason and R. F. Porter, *ibid.*, **68**, 1443 (1964).